Copy No. 2

National Aeronautics and Space Administration
Washington 25, D. C. 20546

29 September 1964

Project Title: Basic Studies on Vortex Stabilized Radiation Sources for Improved Solar Simulation

Contract Number: NASw-858

Contractor: Plasmadyne Corporation
3839 South Main Street
Santa Ana, California

Type of Report: Third Quarterly Status Report
3QS094-858

Period Covered: 3 June 1964 - 18 September 1964

Gentlemen:

1.0 Introduction

The work of this contract is directed toward improving simulation of the solar spectrum (as observed in space) by injecting additives into a gas vortex stabilized radiation source. Additional work with powder additives and energy level studies were conducted during the report period. Argon gas was used exclusively as the carrier gas, however, the energy level studies indicate that krypton or xenon may give better results in some cases. An experimental study on the effect of a small percent of hydrogen in argon was made at 25 KW arc input power.

2.0 Experimental Hardware Improvement

The powder feeding device which was in use during the previous report period has been replaced by the powder feeder shown in Figure 1. This powder feed device consists of a rotating drum (A) into which the powder to be fed (B) is placed. Small quantities of powder fill the tangential

holes drilled thru the drum wall (C) and are carried around to the outlet port (D) where the carrier gas (which is fed into the inside of the drum (E) forces the powder out of the hole and carries it to the arc chamber. The device has two major advantages over the previous feeder.

1. The tangential metering holes are positively emptied by the carrier gas flowing thru them.

2. Powder is continuously prevented from packing and subsequent clogging by the tumbling action of the rotating drum.

A substantial improvement was made on the method of injecting additive powders into the arc. Injection of the powders directly into the arc (i.e. on arc centerline) caused arc operation instability due to the cold carrier gas forcing it off the centerline. This instability problem was eliminated with the electrode and injection device shown in Figure 2. This device operates in the following manner; suspended powder and carrier gas enter the injector electrode at (C) and are accelerated to a high velocity at (A) due to the constricting section, the carrier gas is then bled off at point (D) and returned to the low pressure side of the argon circulation pump. The high velocity imparted to the powder particles at point (A) is sufficient to carry them through (B) and into the arc core. This means that the cold carrier gas is not allowed to pass through orifice (B) disturbing the arc. Experimental work was conducted on this device with the carrier gas flow and carrier gas bleed flow was set slightly higher than the carrier gas flow. This would mean that gas flow to make up the difference would have to flow out of the bulb through orifice (B) against the incoming powder. However, in spite of this bucking gas flow the momentum of the powder carries it into the arc.

3.0 Spectroscopic Instrumentation Techniques

In order to determine the line radiation profiles and examine line broadening, auxiliary instrumentation was set up. This equipment consists of a Tektronix 533 oscilloscope and a Polaroid camera in place of an x-y recorder to record data. The advantage of using the oscilloscope

over the x-y recorder is in its ability to respond to high frequency. The entire system consists of the Bausch & Lomb 250 mm monochromator with RCA 1P-28 or 7102 photomultiplier detectors. The detector output is placed directly on the y axis of the scope and the x axis sweep is controlled by a potentiometer attached to the movable grating of the monochromator. This potentiometer can be adjusted to drive the x axis sweep from zero to full scale covering 100 angstroms. This would mean that any 100 angstrom increment in the spectrum can be accurately investigated for line structure and broadening effects, etc. Initial exploitation of this method is shown in Figure 3, however, here the increment is quite large from .35μ to .55μ.

An addition to the monochromator optics was made, to facilitate obtaining arc radial profiles. Referring to Figure 8 of the Second Quarterly Report, the 46 cm focal length mirror was mounted on a long arm which is rotated slowly by a fine screw thread. The position of this arm is monitored by a 10 turn potentiometer whose output is fed to the x axis input of the x-y recorder. The rotation of the mirror then moves the arc image over the entrance slit of the monochromator thus allowing a scan of the radiation originating in different portions of the arc.

4.0 Argon Vortex Arc Studies

The Second Quarterly Status Report pointed out that a curve of number density of argon atoms and electrons in the argon vortex core plotted against energy level must show a pronounced peak near 11.8 ev or 95,000 cm^{-1}, the energy of argon's resonance transition. It was then to be expected that the effectiveness of any additive atom toward modifying the argon spectrum would depend on how closely a desired excitation level matched the energy levels in the argon arc. A study of all atoms listed in the publication "Atomic Energy Levels" Circular 467, of National Bureau of Standards showed that only a few atoms have promise of causing a useful addition to or modification of the argon vortex spectral distribution when the objective of more closely approximating the solar spectrum is considered. These atoms are hydrogen, barium and mercury.

4.1 Hydrogen

Hydrogen is particularly interesting as can be seen from Figure 4 "Energy Levels - Argon vs Hydrogen". All energy levels of hydrogen should be highly excited. Radiation from the 3 to 2 transitions, Balmer α, at 0.6563μ would be particularly useful in filling the relatively low spectral energy region in the argon spectrum at these wavelengths. Figures 5 and 6 "Spectral Distribution: Hydrogen - Argon Vortex" taken using 10% hydrogen at 11 KW input power and 11 atmospheres pressures are quite instructive. Balmer α line radiation is much more intense than that of nearby argon transitions and shows a large amount of broadening. The half intensity line width is about 9 mμ. The line shape is then fairly well resolved by the 0.46 mμ bandwidth used. The Balmer β line, 0.4861μ is also strong. However, the Balmer γ line, 0.431μ is not evident. This may be due to stripping of electrons from the higher term levels as has been noted in argon. The results obtained were sufficiently interesting to justify a 25 KW run comparing argon and 5% H_2 95% argon vortex radiation with the spectral distribution of solar radiation in space. Figure 7 gives the results. The characteristic ultraviolet excess and visible deficiency of argon is clearly evident. 5% hydrogen causes a general decrease in radiative efficiency except around .656μ where the output increases. It can also be seen that near 0.486μ the 5% H_2 output is nearly equal to the original argon curve. The 5% H_2 - 95% argon curve is a better match of solar radiation than pure argon. It is likely that higher hydrogen percentages would produce an even better match but only with additional loss in total radiative efficiency. However, the evaluation of light source radiative efficiency must consider the spectral transmission of the solar simulation system. It is entirely possible that hydrogen-argon mixtures will have improved system efficiencies even though the total radiative efficiency of the source decreases.

The use of krypton instead of argon has been considered. Krypton has a 4p ground state, 5s resonance at 81,000 cm^{-1}, 5p levels from 91,000 cm^{-1} to 94,000 cm^{-1} and ionization potential at 14.0 volts. These levels are compatible with hydrogen and efficient excitation of Balmer α and β lines is expected. The krypton-hydrogen mixtures should have

less vacuum ultraviolet than argon. The atomic cross section of krypton for electrons is considerably greater than that of argon, and the radiation processes should be more efficient.

The use of xenon with hydrogen mixture has been studied by Thouret and Strauss (1) in compact arc lamps. They note that the excitation levels of hydrogen are higher than those of xenon. For example, the ionization potential of xenon is 12.1 volts or 97, 800 cm^{-1} while the 3rd quantum level of hydrogen is 97, 500 cm^{-1} and the 4th at 102, 800 cm^{-1}. Some Balmer α radiation can be expected but excitation can not approach the extent likely with argon and krypton. Although hydrogen does not substantially participate in the excitation and ionization processes of the short arc lamps, hydrogen-xenon mixtures merit study in the vortex arc with its higher excitation potentials if the addition of radiation at wavelengths near 0.656μ proves to be desirable.

The addition of hydrogen for the purpose of further constricting the inert gas vortex arcs would serve no useful purpose. Essentially, the radial dimension of an arc is controlled by the mean free path of electrons throughout the arc volume. The mean free path is inversely proportional to the product of the atomic number density of the arc gas and its electron collision cross section. As the vortex flow maintains a cool high density gas very close to the arc axis, electron mean free path decreases very rapidly as an electron moves out from the arc core. The addition of molecular hydrogen with its large cross section may have some effect but this was not apparent with the 25 KW run. The number density in a typical argon vortex at about 2 mm from the arc axis (just outside the arc) is believed to be $\approx 3.5 \times 10^{20}$ cm^{-3} operating with $\approx$ 15 atmospheres input pressure. At this same location the number density of 5% hydrogen would be 1.8×10^{19} cm^{-3}. Considering electrons of 4 ev energy argon's elastic collision cross section is 7.5×10^{-16} cm^2 while molecular hydrogen's is 14×10^{-16} cm^2. The product of number density times cross section or number of collisions per centimeter would then compare as 2.6×10^5 cm^{-1} for argon to 2.5×10^4 cm^{-1} for molecular hydrogen making argon the more important constricting gas. At lower energies the effect of 5% hydrogen

becomes more important being about equal to argon at one electron volt and less. It is interesting to note that assuming an atomic temperature of argon at around 28,000°K (about 2.4 ev) in the arc core the atomic number density there would be $\approx 3.5 \times 10^{18}$ cm^{-3} and the number of elastic collisions per centimeter for 4 ev electrons would be 2.6×10^{3}. This number would increase by a factor of 3 as electron energies continue to increase under the arc gradient to 12 - 14 ev where inelastic collisions become important. It is very evident that electron mean free path in the vortex arc is probably 100 times greater along the arc axis than it is approximately 2 mm from the axis in the cool vortex flow. The presence or absence of hydrogen does not appreciably change this condition.

4.2 Barium

The spectral distribution of the argon vortex with barium as an additive was discussed in the Second Quarterly Report. The energy level diagram, Figure 8, can be used to explain the radiation curves of Figure 12, and Figures 17, 18 and 19 of the Second Report. As was previously reported barium I lines are weak while the barium II lines are strong and well broadened. The strongest lines are around 0.455μ, 0.493μ, 0.413μ, and 0.389μ. These lines are indicated on the energy diagram. In solar simulation applications where large wavelength bands, say 50 or 100 mμ, are permissible the argon-barium vortex could be very effective.

The radiation of barium in the vortex arc is quite different from its emission in mercury vapor-metallic iodide arc lamps as reported by Reiling (2). In a 400 watt lamp with barium iodide as an additive the strongest barium lines are 0.5535μ, 0.6142μ, 0.6498μ, 0.6595μ, 0.7059μ, 0.7280μ, 0.7673μ, and 0.8560μ, all from barium I. The lowest energy level barium II line at 0.4554μ is also present. It is very clear that the excitation energies prevailing in the argon vortex arc are far higher than in the mercury arc lamp.

4.3 Titanium

Figure 10 of the Second Quarterly Report presented the spectral distribution of the argon-titanium vortex. Figure 9 of this report gives the corresponding energy level diagram of titanium and compares it with argon. Like hydrogen, titanium II energy levels overlap those of argon and strong excitation occurs. Many 4p - 4s transitions are possible with wavelengths starting at about 0.335μ and extending to shorter wavelengths. The argon-titanium vortex is then a strong source of ultraviolet and while not pertinent to the solar simulation problem it offers insight as to the physics of additives to the argon vortex.

4.4 Bromine

Figure 10 sketches the energy levels of bromine. This diagram is presented as the salts studied are often compounds of bromine. 6p - 6s and 5p - 5s transitions should produce observable radiation, however, bromine lines have not been noted as yet.

4.5 Mercury

The argon vortex has been operated with direct injection of mercury vapor and by injection of mercuric bromide as a powder. Adequate spectral distribution data is not yet available due to operating difficulties.

Figure 11, Energy Levels - Argon vs Mercury, points out that mercury will be easily ionized in the argon vortex but also that fairly strong radiation should occur near 0.579μ, 0.577μ, 0.546μ, 0.405μ, and 0.365μ. Unwanted ultraviolet radiations at 0.185 and 0.254μ will, of course, also occur. Mercury would be even more compatible with the krypton vortex. The line radiations between 0.546μ and 0.579μ provide a spectral fill in a deficient region for argon, hydrogen-argon and krypton. Additional experimental work will be done with the injection of mercury into the argon vortex.

5.0 Profile Study Sodium - Argon Vortex

The profile instrumentation discussed in Section 3.0 was first used to study the argon vortex with injected sodium cloride. As is evident in Figure 12 of the Second Quarterly Report sodium line radiation is relatively weak. This is due to the formation of ionized sodium in the argon vortex. Assuming that this conclusion is correct sodium radiations should occur as a halo or cylindrical shell around the arc core in the relatively cool surrounding vortex gas. Visual observation of a sodium injected argon vortex substantiates this expectation. A cylindrical halo of brilliant yellow does surround the arc vortex.

Figure 12 gives the first profile taken in study of this halo used a grating monochromator set at 0.589μ and with a bandwidth of 2 mμ. The slit in terms of arc dimensions had a width of 0.5 mm and a height of 8 mm. The length of the arc was 14 mm and the long dimension of the slit was parallel to the axis of the arc. The two profiles sketched give the argon vortex arc profile before and after injection of sodium. With sodium being added a shell with about 1 mm thickness centered near 2 mm in radius from the arc axis is radiating almost entirely from sodium.

This first data must now be expanded by additional experiments. The spectral distribution of radiation from the halo must be determined. The profile must be retaken at 0.589μ and then be repeated without changing arc power or powder feed at a nearby wavelength which is weak in the profile. These data should resolve a number of interesting questions. Such as, is the halo radiation resonance fluorescence or is it caused by collisional excitation? The mobility of the sodium ion with atomic weight of 23 in argon is somewhat greater than the mobility of the argon ion with atomic weight of 40. This data is referenced by Brown (3). The existance of a uniform sodium shell around the arc may be related to this greater ion mobility.

6.0 Planned Work

The following experimental work should be accomplished during the last phases of the contract.

Data should now be obtained on micro spectral radiance of the more promising vortex arcs. This will be done by comparison with a calibrated tungsten filament.

Vortex profile studies should be extended from sodium to mercury and also to hydrogen when it is introduced as a portion of the injection compound. This profile work should be pushed into the vacuum ultraviolet. For example, mercury's resonance line at 0.1850μ should be observed.

The radiation of possible optimum combinations of barium, mercury and hydrogen to the argon vortex should be compared with the solar spectrum.

On completion of the various phases of the experimental work the physical description of the vortex arc with minority additives can be more correctly stated.

7.0 Funds Expended

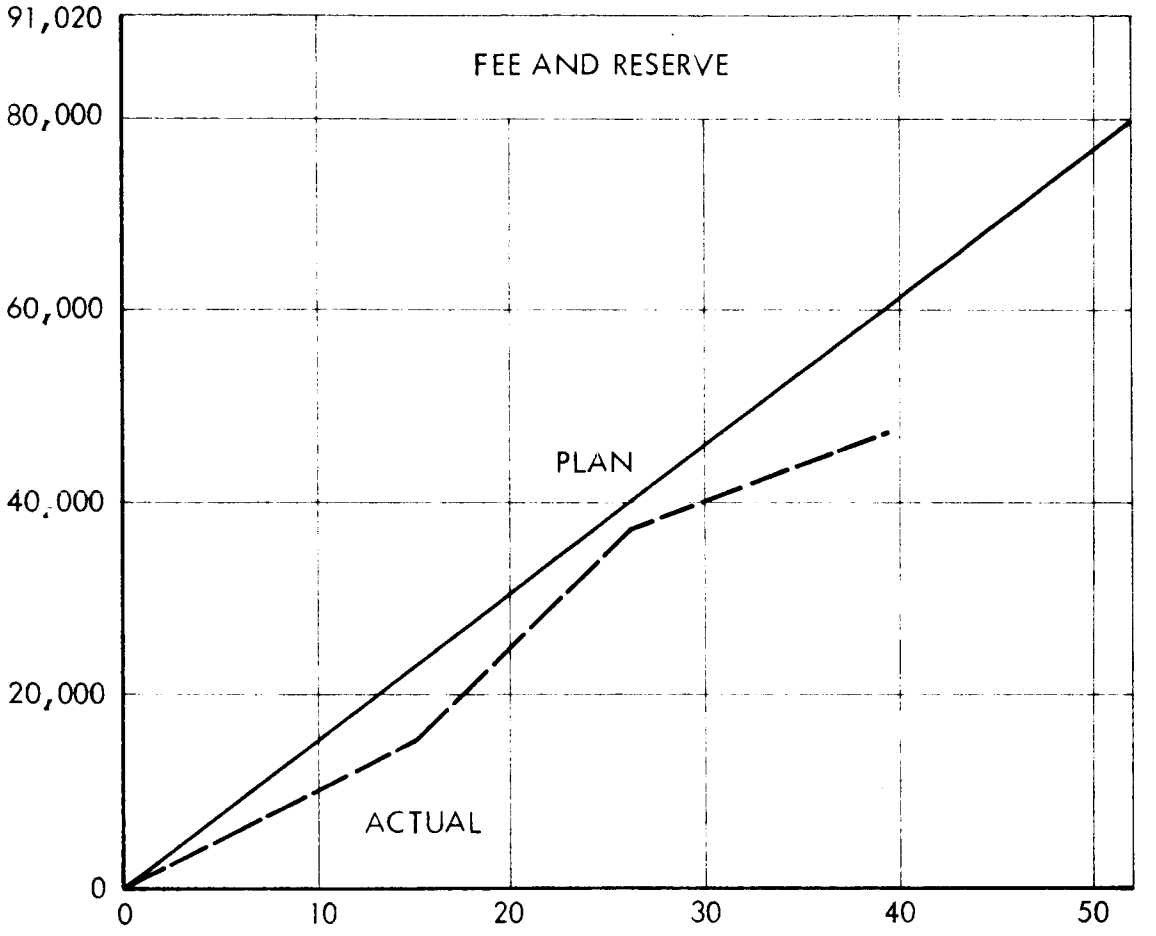

Contract initiated 3 December 1963 - End 39th Week 6 September 1964

Prepared by:

Ronald E. Sheets
Test Engineer
Optical Group

Delbert G. Van Ornum
Senior Scientist
Optical Group

8.0 References

1. Thouret, W. E. and H. S. Strauss 1963: Xenon Compact Arcs with Increased Brightness Through Addition of Hydrogen. Illuminating Engineering, Vol. 58, No. 5, p. 37 (May 1963).

2. Reiling, G. H. 1964: Characteristics of Mercury Vapor - Metallic Iodide Arc Lamps. J. Opt. Soc. Am. Vol. 54, No. 4, p. 532.

3. Brown, S. C. 1959: Basic Data of Plasma Physics. New York, John Wiley and Sons, p. 75 and p. 78.

9.0 List of Figures

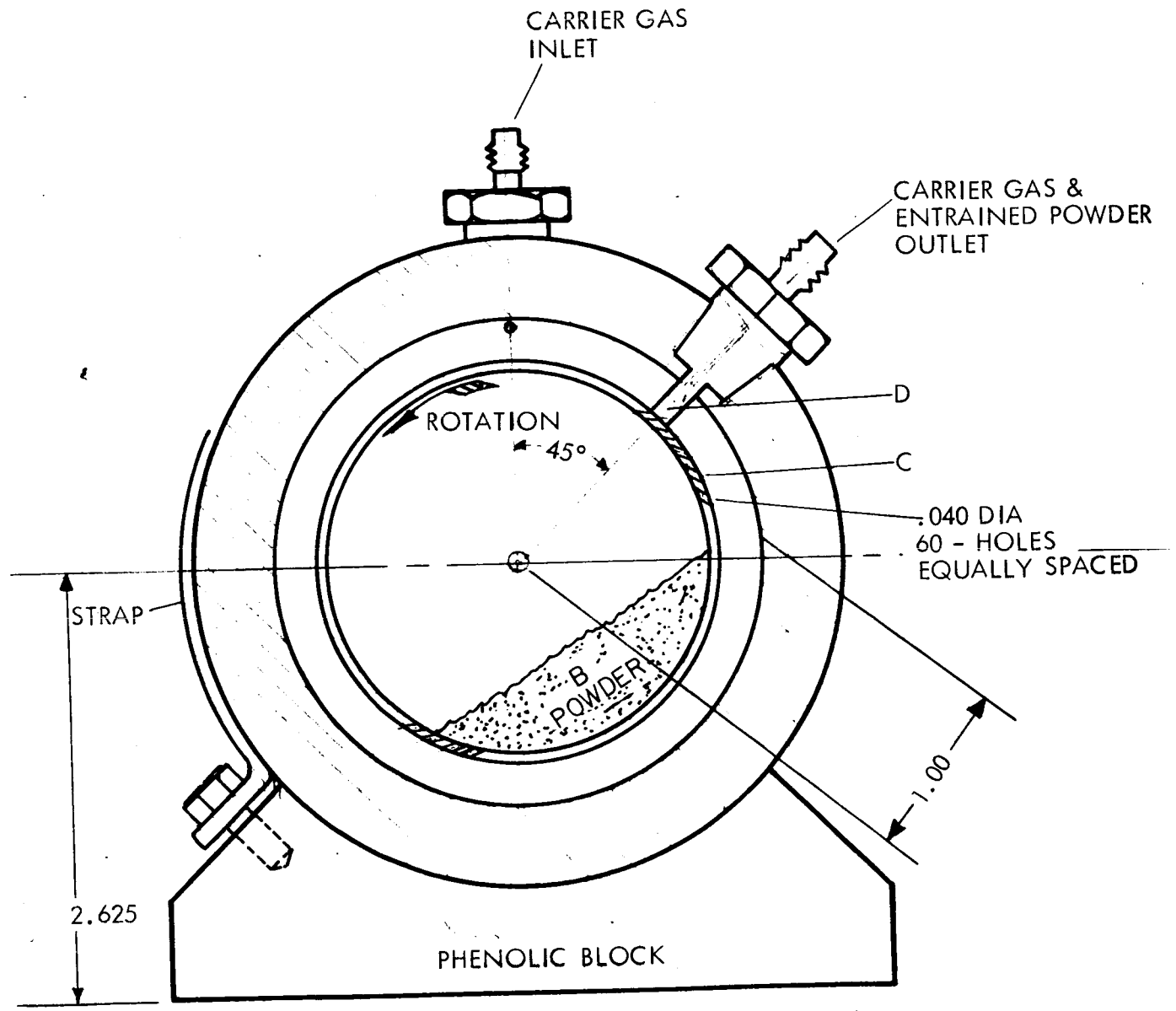

SECTION A - A

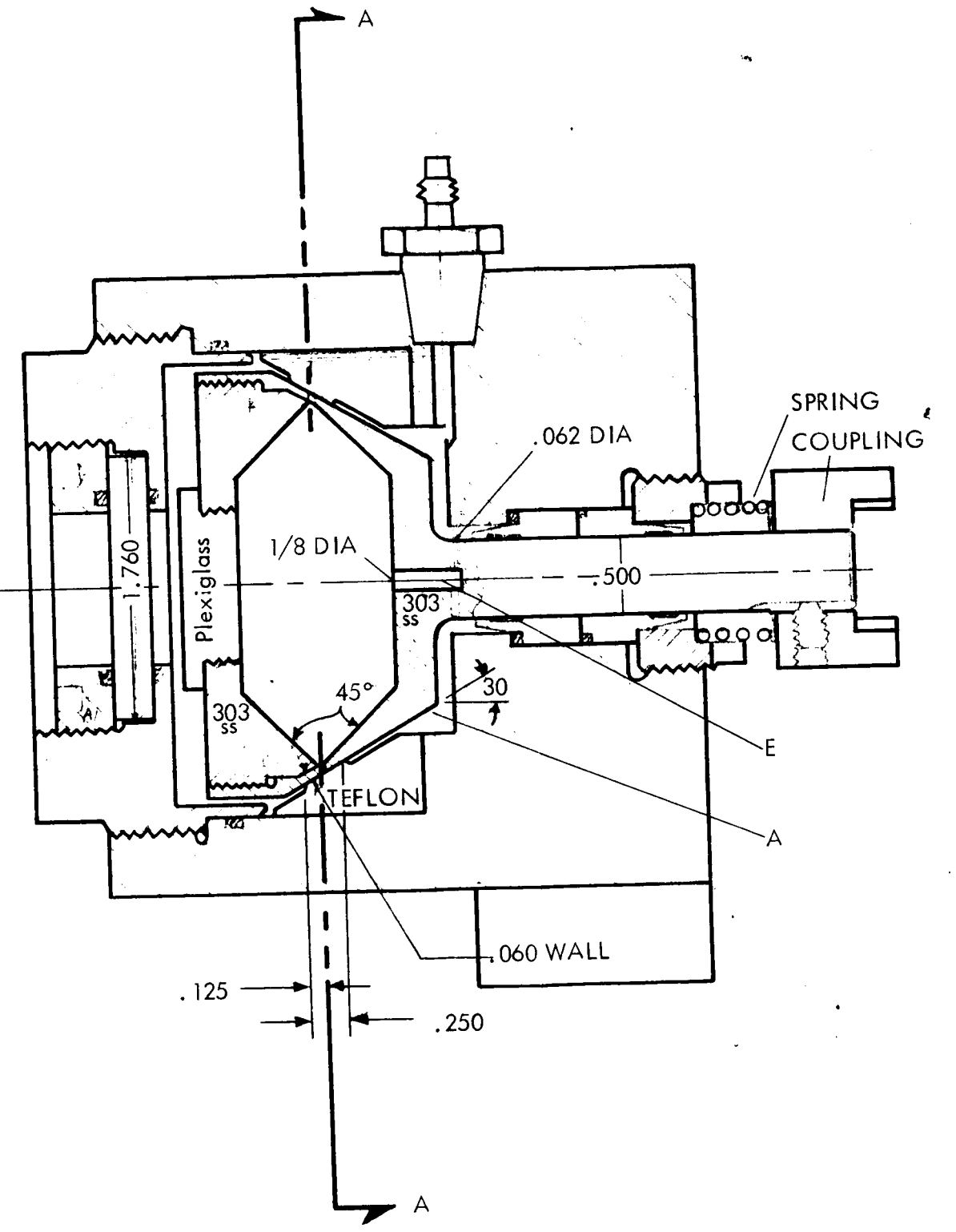

FIGURE 1 - POWDER FEED DRUM

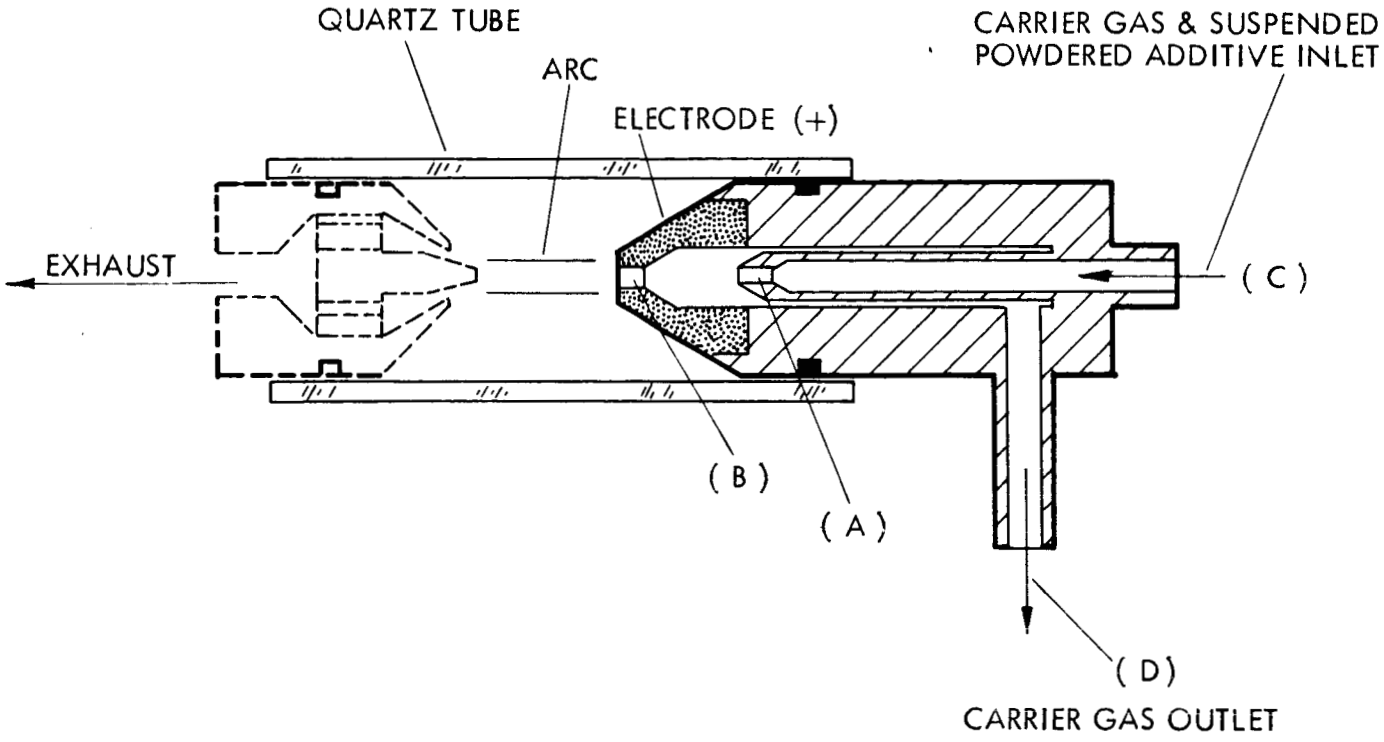

FIGURE 2 - POWDER INJECTING ELECTRODE

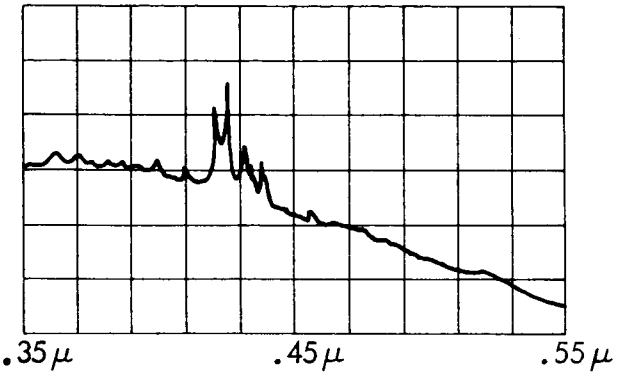

FIGURE 3 - ARGON SPECTRUM WITH S-5 DETECTOR

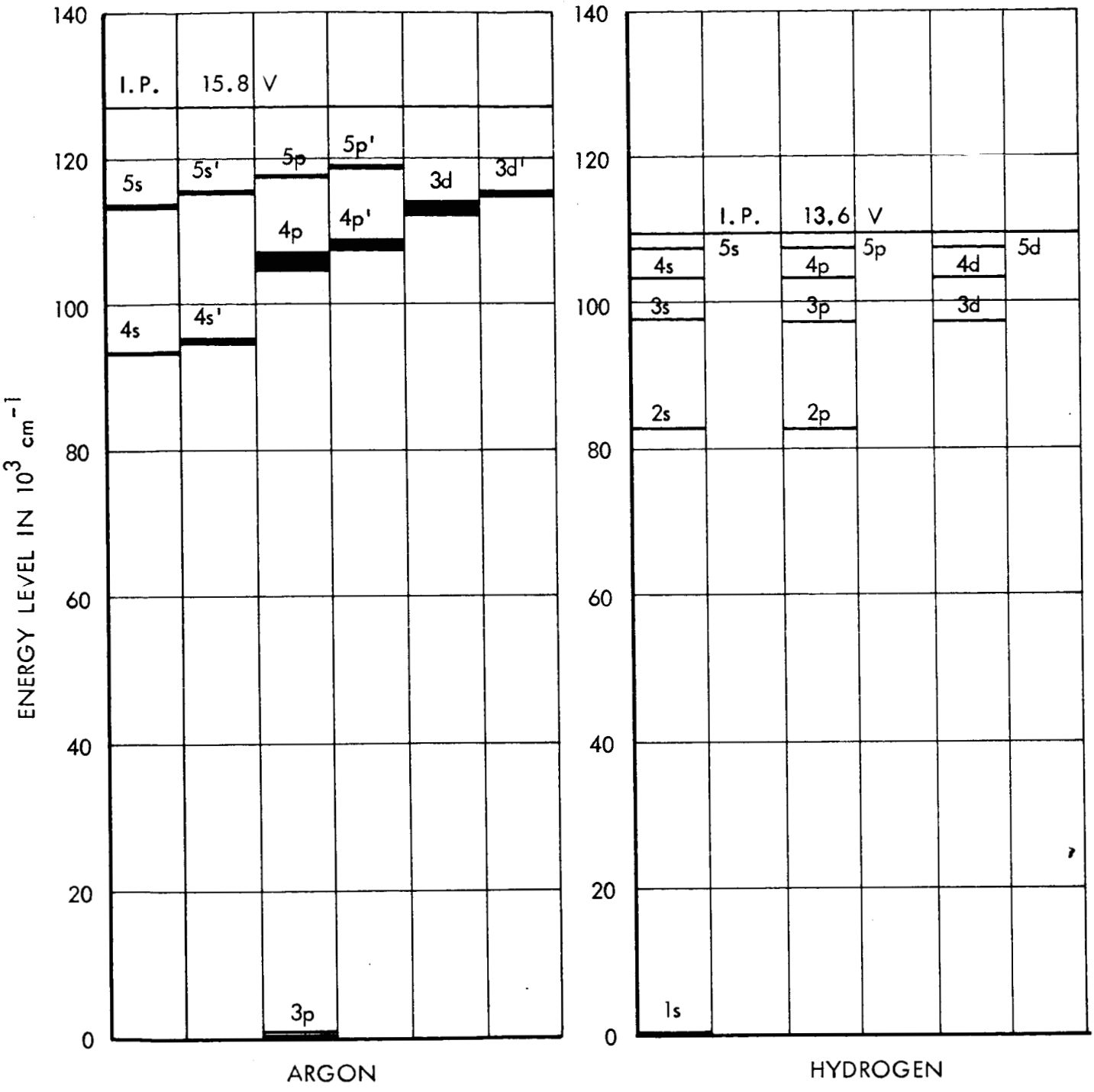

FIGURE 4 - ENERGY LEVELS - ARGON VS HYDROGEN

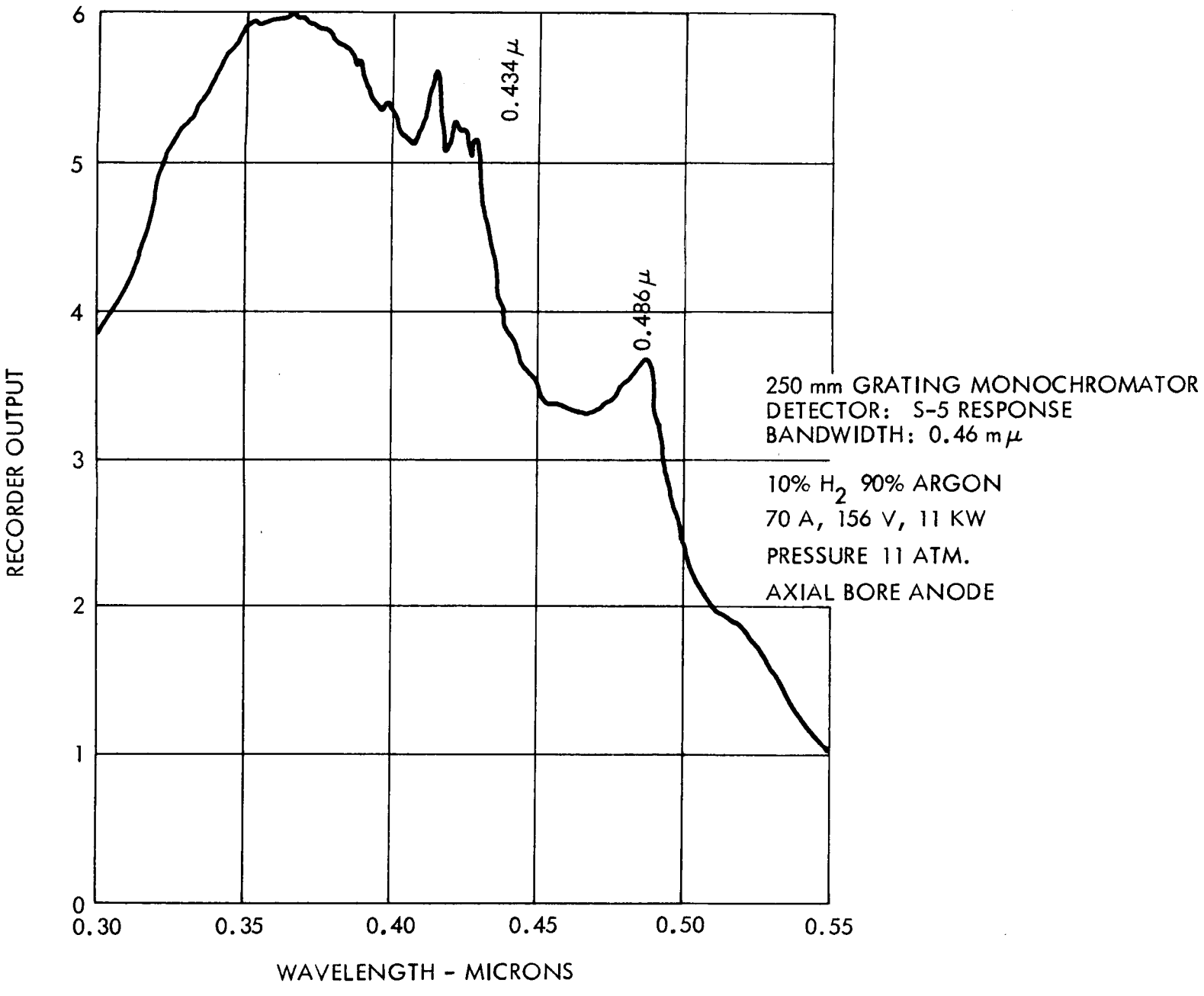

FIGURE 5 - SPECTRAL DISTRIBUTION: HYDROGEN - ARGON VORTEX

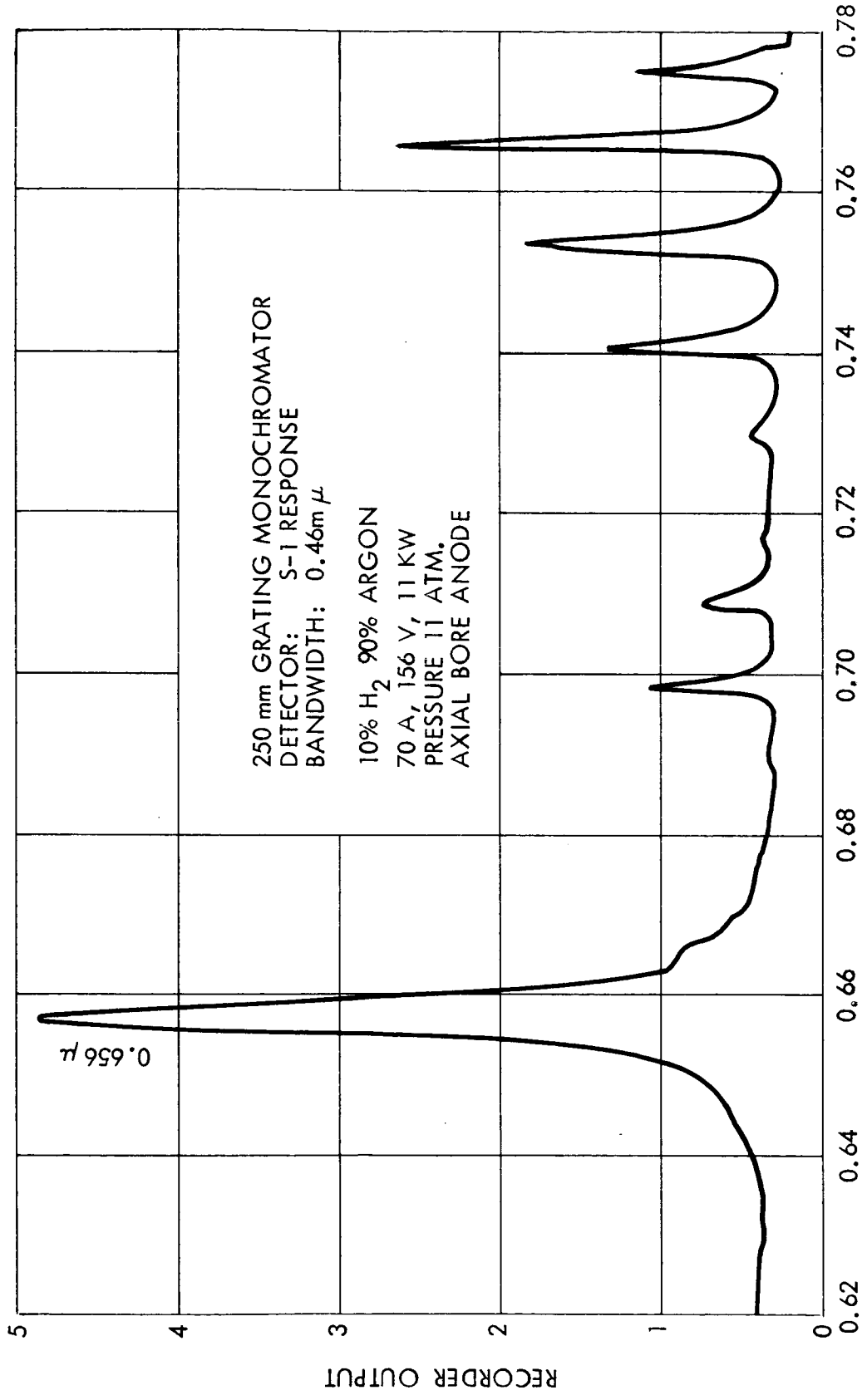

FIGURE 6 - SPECTRAL DISTRIBUTION: HYDROGEN - ARGON VORTEX

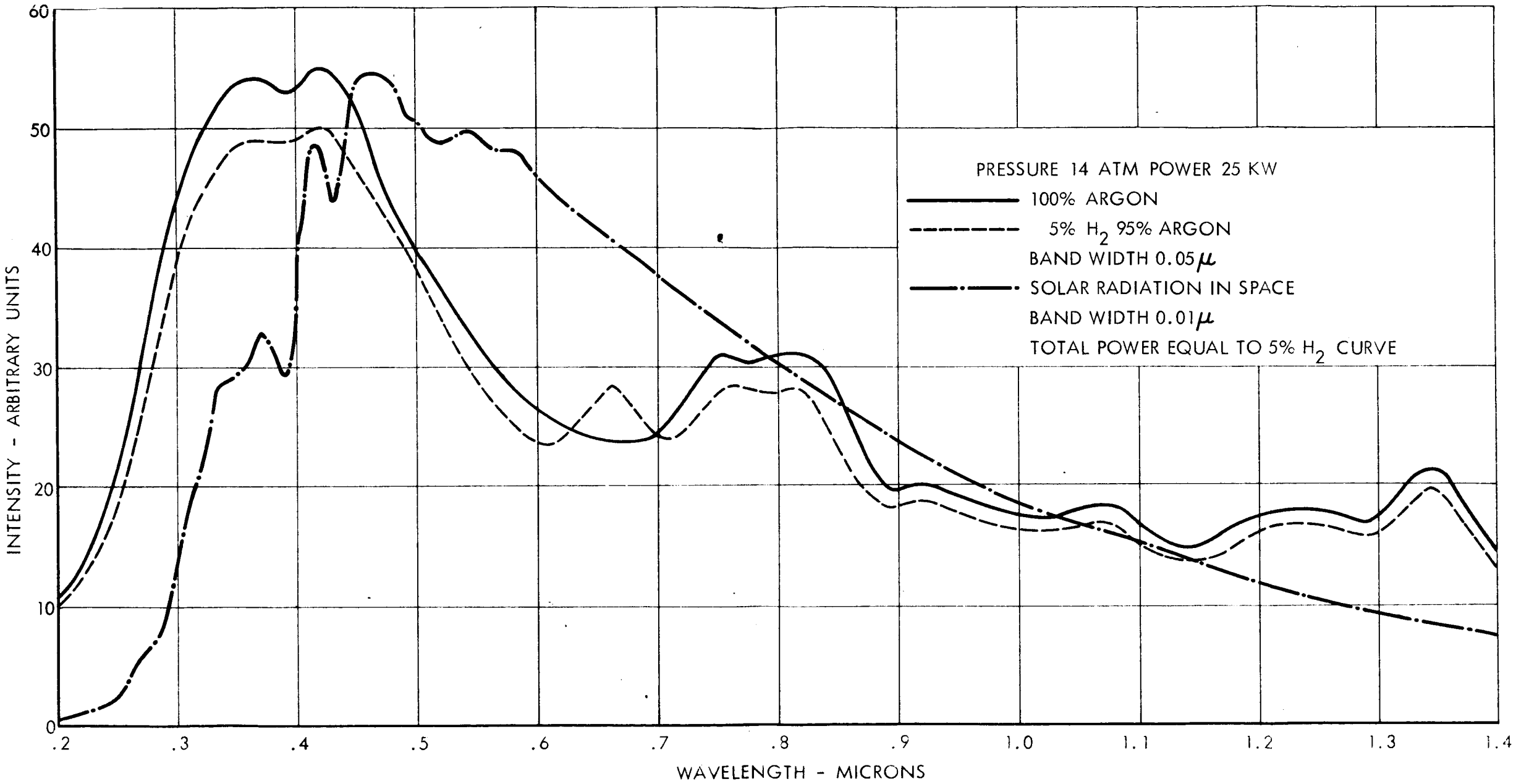

FIGURE 7 - SPECTRAL DISTRIBUTION VORTEX RADIATION VS. SOLAR RADIATION

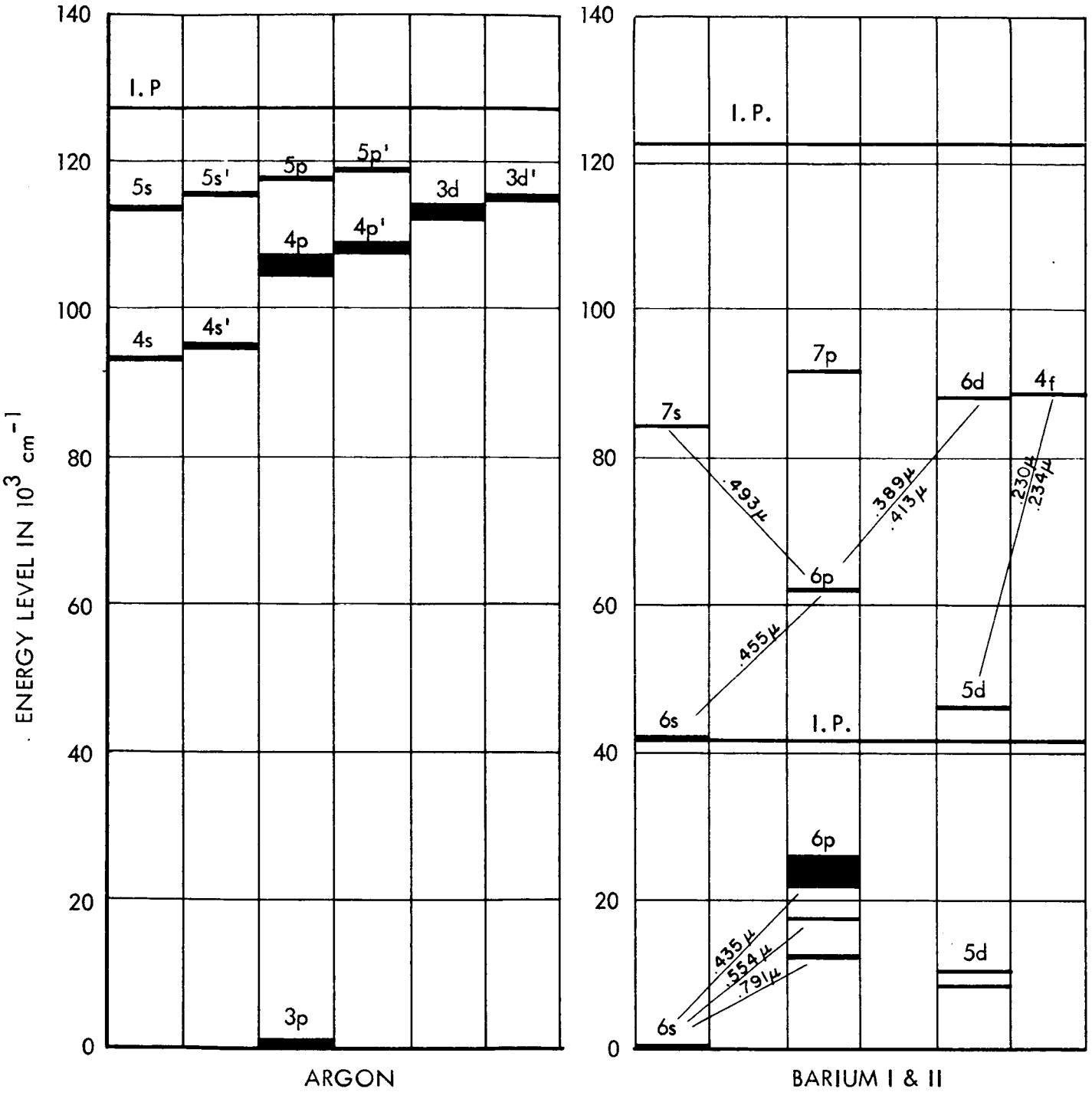

FIGURE 8 - ENERGY LEVELS - ARGON VS BARIUM

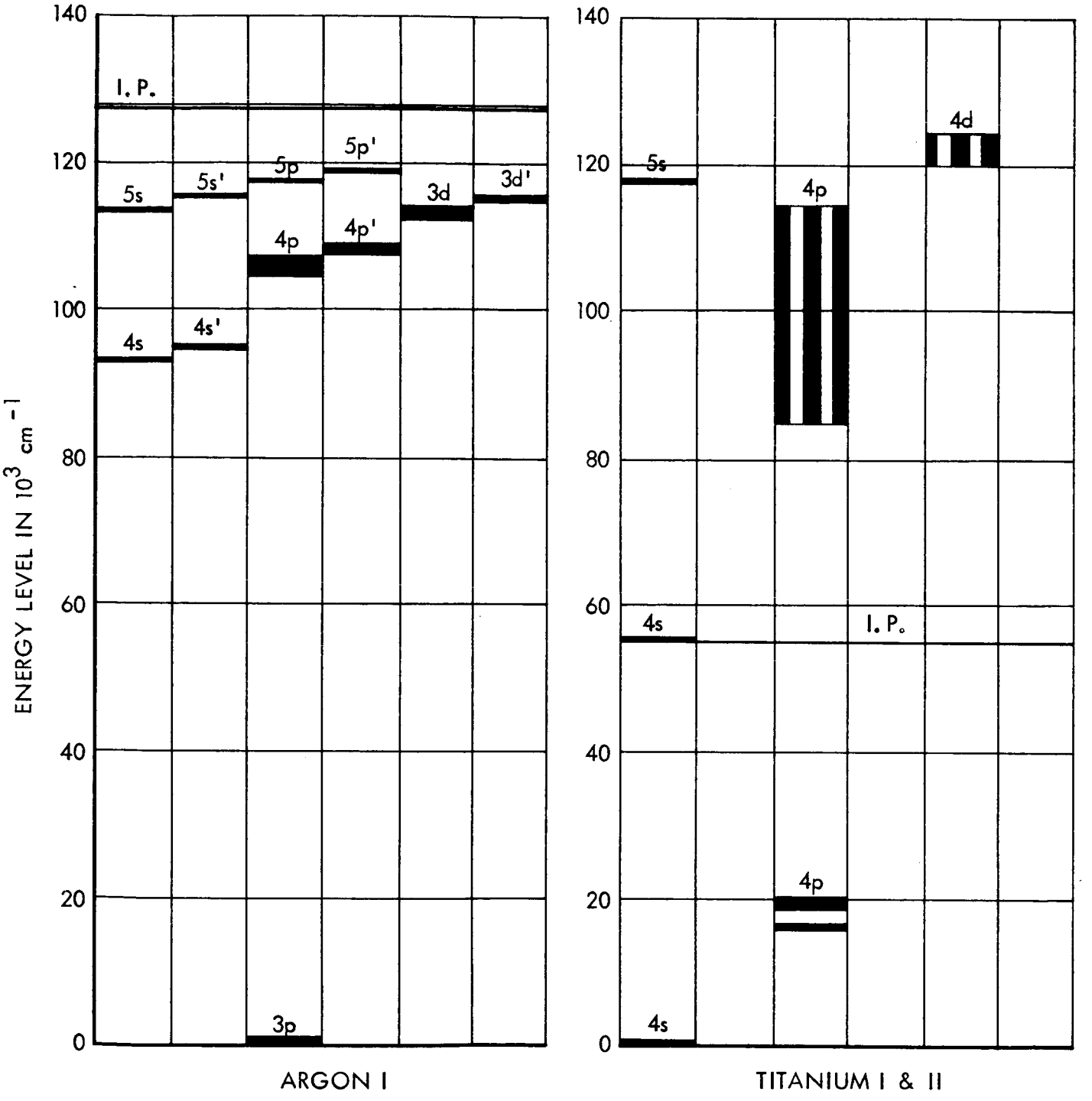

FIGURE 9 - ENERGY LEVELS - ARGON VS TITANIUM

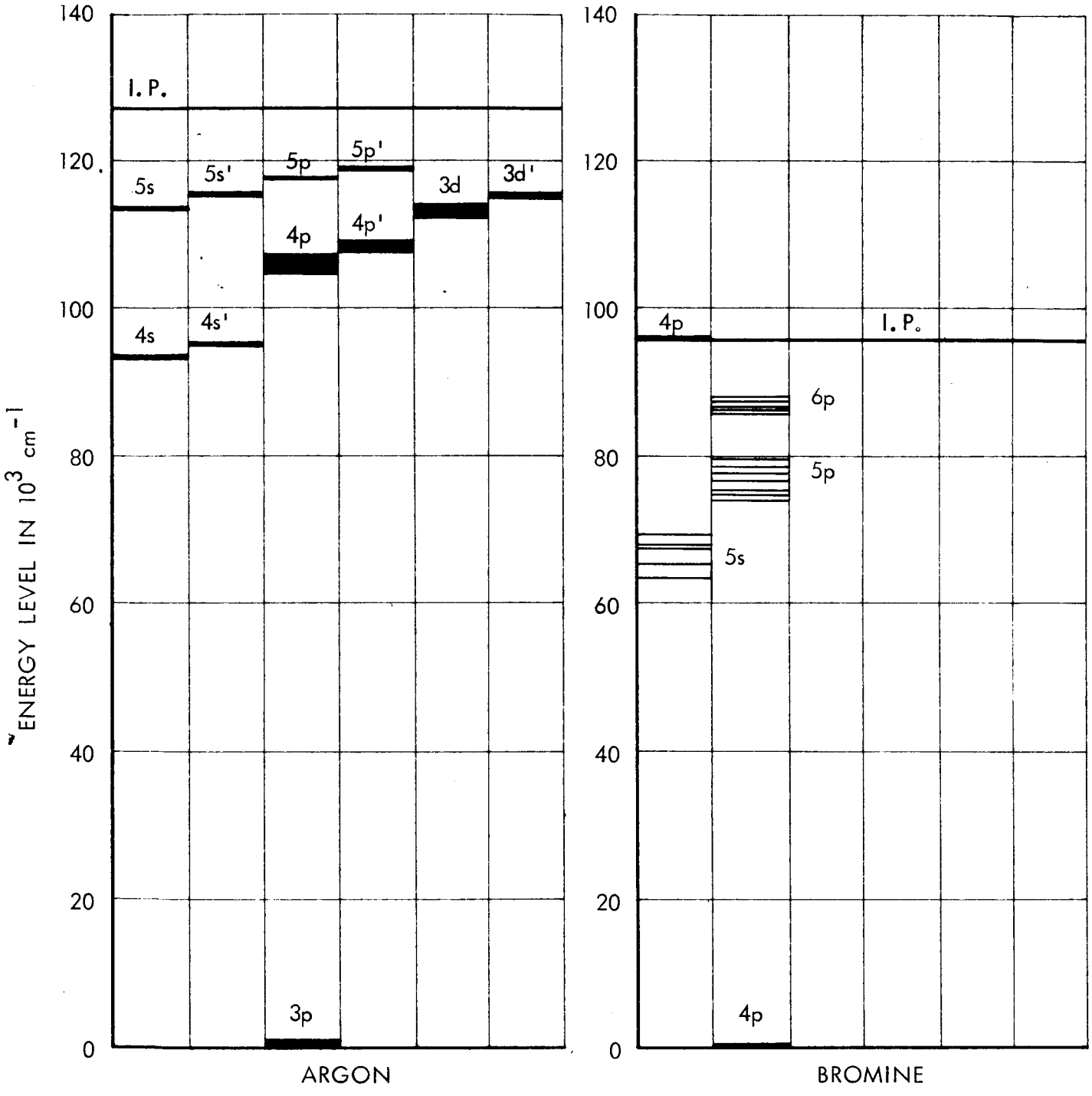

FIGURE 10- ENERGY LEVELS - ARGON VS BROMINE

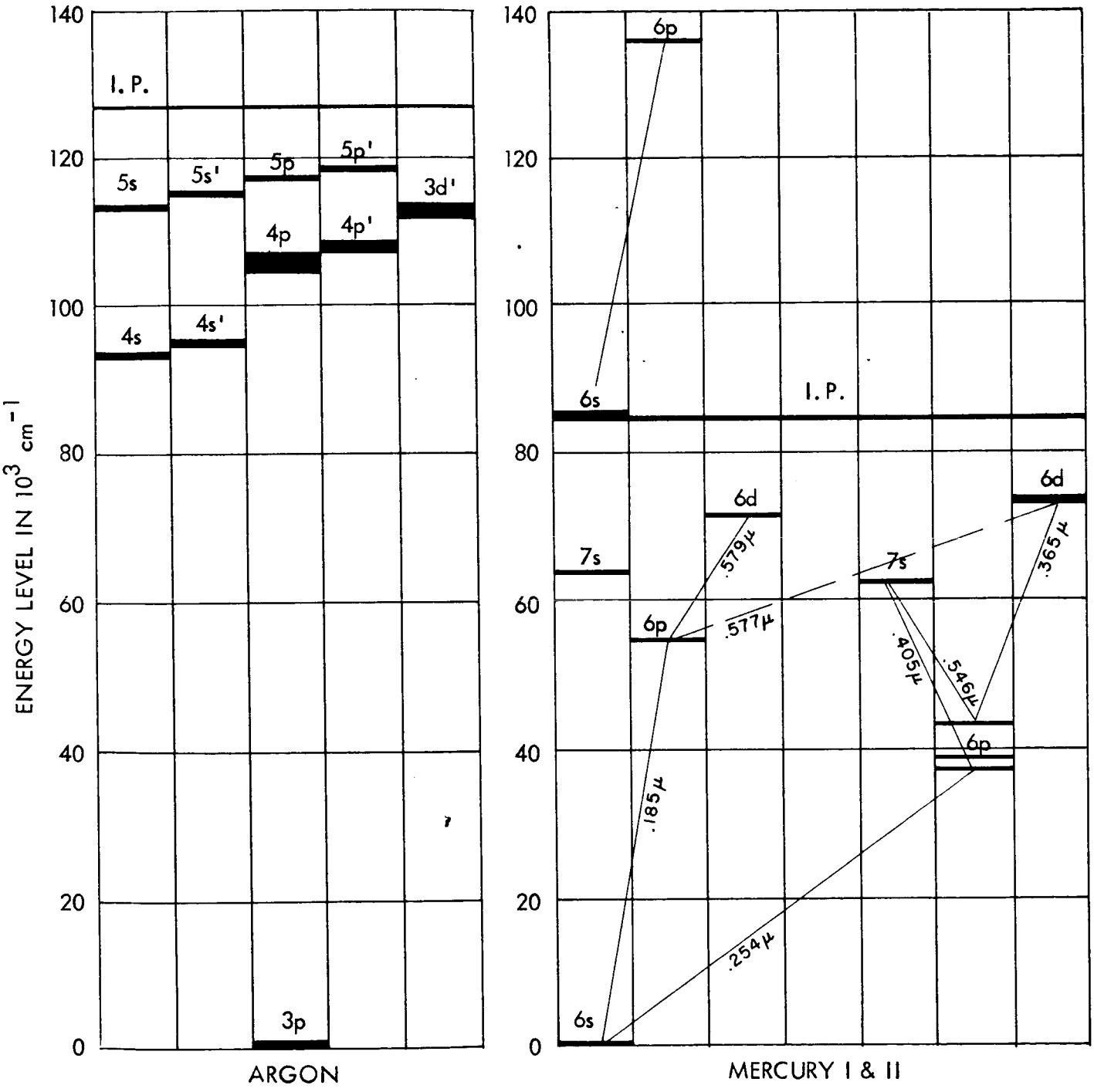

FIGURE 11- ENERGY LEVELS - ARGON VS MERCURY

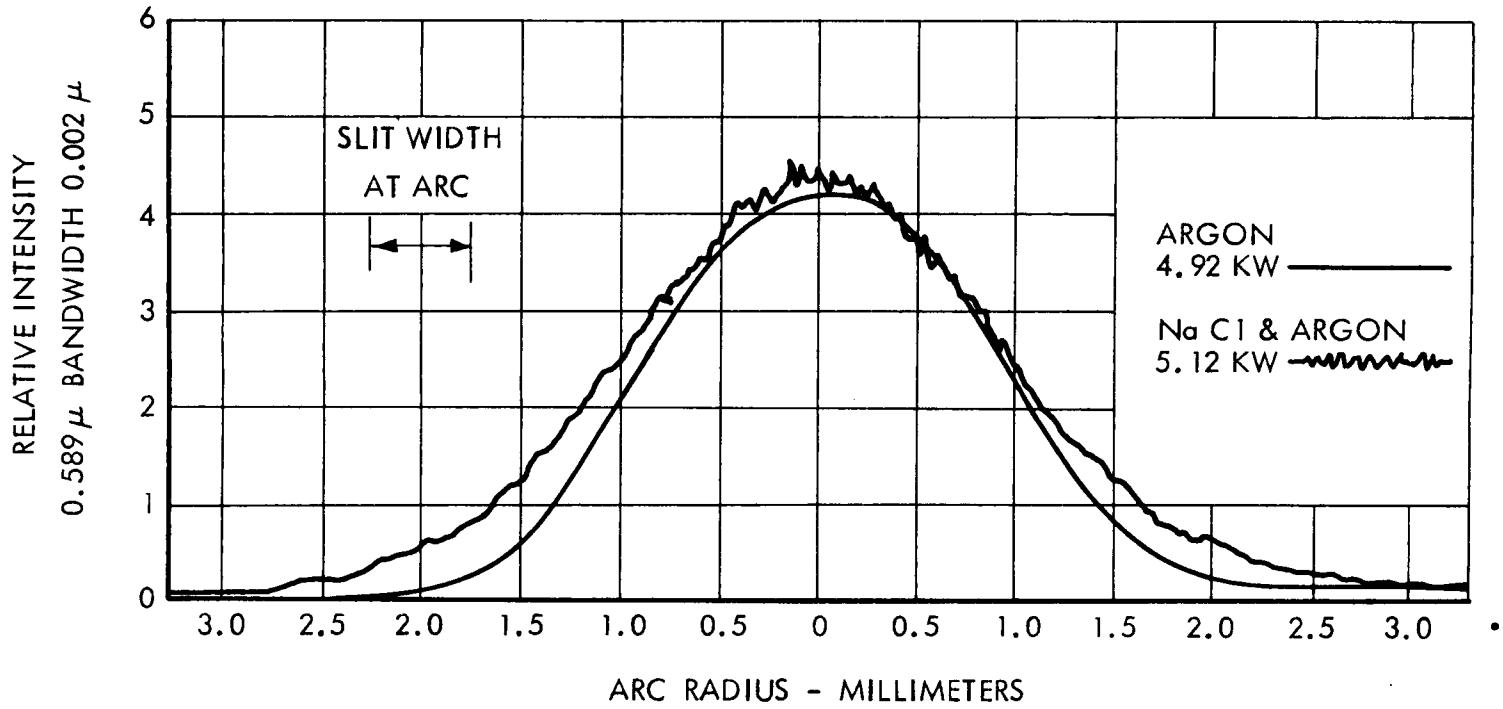

FIGURE 12- PROFILE SODIUM VORTEX RADIATION